materials

MDPI

Article

Surfactant-Assisted Synthesis of Micro/Nano-Structured $LiFePO_4$ Electrode Materials with Improved Electrochemical Performance

Yuqing Qiao [1], Ying Liu [1], Jianguo Zhu [1], Peng Jia [1,*], Liqiao Zhang [1], Wei Zhou [1] and Tifeng Jiao [1,2,*]

[1] Hebei Key Laboratory of Applied Chemistry, School of Environmental and Chemical Engineering, Yanshan University, Qinhuangdao 066004, China
[2] State Key Laboratory of Metastable Materials Science and Technology, Yanshan University, Qinhuangdao 066004, China
* Correspondence: pengjia@ysu.edu.cn (P.J.); tfjiao@ysu.edu.cn (T.J.)

Abstract: As an electrode material, $LiFePO_4$ has been extensively studied in the field of energy conversion and storage due to its inexpensive cost and excellent safety, as well as good cycling stability. However, it remains a challenge to obtain $LiFePO_4$ electrode materials with acceptable discharge capacity at low temperature. Here, micro/nano-structured $LiFePO_4$ electrode materials with grape-like morphology were fabricated via a facile solvothermal approach using ethanol and OA as the co-solvent, the surfactant as well as the carbon source. The structure and electrochemical properties of the $LiFePO_4$ material were investigated with x-ray diffraction (XRD), field emission scanning electron microscopy (SEM), cyclic voltammetry (CV) and electrochemical impedance spectroscopy (EIS), and the formation mechanism of the self-assembled micro/nano-structured $LiFePO_4$ was discussed as well. The micro/nano-structured $LiFePO_4$ electrode materials exhibited a high discharge capacity (142 $mAh{\cdot}g^{-1}$) at a low temperature of 0 °C, and retained 102 $mAh{\cdot}g^{-1}$ when the temperature was decreased to −20 °C. This investigation can provide a reference for the design of micro/nano-structured electrode materials with improvement of the electrochemical performance at low temperature.

Keywords: li-ion batteries; $LiFePO_4$; oleic acid; cathode material

check for updates

Citation: Qiao, Y.; Liu, Y.; Zhu, J.; Jia, P.; Zhang, L.; Zhou, W.; Jiao, T. Surfactant-Assisted Synthesis of Micro/Nano-Structured $LiFePO_4$ Electrode Materials with Improved Electrochemical Performance. *Materials* **2022**, *15*, 8953. https://doi.org/10.3390/ma15248953

Academic Editor: Enrico Negro

Received: 2 November 2022
Accepted: 12 December 2022
Published: 14 December 2022

Publisher's Note: MDPI stays neutral with regard to jurisdictional claims in published maps and institutional affiliations.

Copyright: © 2022 by the authors. Licensee MDPI, Basel, Switzerland. This article is an open access article distributed under the terms and conditions of the Creative Commons Attribution (CC BY) license (https://creativecommons.org/licenses/by/4.0/).

1. Introduction

Due to its high theoretical capacity (170 $mAh{\cdot}g^{-1}$), moderate voltage plateau (3.4 V versus Li^+/Li), long cycling life, environmental compatibility and low cost [1–4], $LiFePO_4$ (LFP) has been intensively investigated as one of the most promising cathode materials for rechargeable lithium-ion batteries used in electric vehicles (EVs) and hybrid electric vehicles (HEVs). However, $LiFePO_4$ cathode material presents the lower li-ion diffusion coefficient (10^{-14}~10^{-16} $m^2{\cdot}S^{-1}$) [5–7] and electronic conductivity (10^{-9}~10^{-10} $S{\cdot}cm^{-1}$) when compared with other cathode materials such as $LiCoO_2$ [8], $Li_3V_2(PO4)_3/C$ [9], $Cu_{0.95}V_2O_5$ [10], FeF_3 [11], V_2O_5 [12]. It is reported that an effective approach to enhance electronic conductivity is to coat conductive materials on the surface of $LiFePO_4$ particles or dope metal-ions/metal-oxide to change $LiFePO_4$ lattice [13–16]. As the li-ion diffusion path (such as diffusion distance and diffusion channel) is predominantly controlled by the diffusion time (diffusion coefficient), nanocrystallization is favorable for improvement of the li-ion diffusion time for the short diffusion distance [17–19]. Peng et al. [20] synthesized a one-dimensional (1D) single-crystalline nanoarchitectures $LiFePO_4$ with good rate capability. Zhao et al. [21] synthesized a two-dimensional (2D) single crystalline $LiFePO_4$ with the highest pore density for lithium-ion insertion/extraction. Xia et al. [22] prepared large-scale $LiFePO_4$ microspheres with a three-dimensional (3D) porous microstructure and these micro/nano-structured $LiFePO_4$ microspheres have a high tap density, which show excellent rate capability and cycle stability as electrodes.

In addition, as one of the most widely used electrode materials of lithium-ion batteries (LIBs) for electric vehicles, $LiFePO_4$ cathode materials possess many excellent properties, including excellent safety [1–4,22–28]. However, the poor discharge capacity at relative lower temperatures (below −20 °C) hinders its practical applications in special environment or regions. Generally, the working temperature of $LiFePO_4$ cathode materials is between −10 and 55 °C. For $LiFePO_4$ cathode materials used at low temperatures, several problems should be considered. First, the specific capacity of $LiFePO_4$ cathode materials will reduce sharply (40~60% at a low temperature of −20 °C); Second, the capacity of $LiFePO_4$ cathode materials will be consumed rapidly at a low temperature. In addition, lithium dendrites will be formed easily when the LIBs are charged at low temperatures, which can pierce the separator between electrodes and cause an inner short circuit [27]. Cao et al. [27] reported that kinetic characteristics of LIBs determine their electrochemical performance at low temperatures. To improve the dynamic properties, a number of $LiFePO_4$ electrode materials with nano scales or with a porous structure have been developed [2,20,22,26].

To date, a number of synthesized methods, such as solid-state techniques [23], hydrothermal synthesis [24], co-precipitation [25], sol-gel reaction [26], as well as other methods with improved electrochemical properties [27,28], have been developed to prepare nano-sized $LiFePO_4$ particles. As a typical surfactant, OA is used as surfactant and template in solvothermal synthesis of $LiFePO_4$ cathode materials. Yang et al. [29] reported that the introduction of OA can lead to a smaller particle size and a homogeneous size distribution of $LiMnPO_4$ particles, resulting in improved electrochemical performance. In addition, Rangappa et al. [30] prepared $LiFePO_4$ cathode materials with a flower-like microstructure using a solvothermal method with ethylene glycol (EG) and OA as co-solvent and surfactant, where the EG and OA played a key role in controlling the size and morphology of $LiFePO_4$ nanocrystals. In addition, the EG and OA also acted as the carbon source when the precursor was carbonized at a high temperature (600 °C). The nano-scaled $LiFePO_4$ cathode materials exhibited a high specific capacity and a good cyclic performance. In this work, micro/nano-structured $LiFePO_4$ electrode materials with grape-like morphology were fabricated via a facile solvothermal approach using ethanol and OA as the co-solvent, the surfactant as well as the carbon source. The micro/nano-structured $LiFePO_4$ electrode materials exhibited a high discharge capacity of 142 $mAh{\cdot}g^{-1}$ at 0 °C, and retained 102 $mAh{\cdot}g^{-1}$ when the temperature was decreased to −20 °C. This investigation can provide a reference for the design of micro/nano-structured $LiFePO_4$ electrode materials with improvement of the electrochemical performance at a low temperature.

2. Experiment

2.1. Materials

$LiFePO_4$ microspheres were synthesized using a facile co-solvothermal method with ethanol, deionized water as the co-solvent and OA as surfactant. All the reagents used for synthesis and experiments were analytical grade and employed as received, without any further purification. First, 40 mL ethanol were added into a beaker and mixed with 20 mL deionized water. Designed amount of OA ($C_{18}H_{34}O_2$, approx. 2.0 mL, Tianjin Kaitong chemical Co., Ltd., Tianjin, China) was added in the mixed solvent and heated to be dissolved. The mixture was separated into two parts evenly (beaker A and beaker B), and then 12 mmol Lithium hydroxide ($LiOH{\cdot}H_2O$ 90%, Tianjin Fengchuan chemical Co., Ltd., Tianjin, China) was added into beaker A, followed by adding 3 mmol phosphoric acid (H_3PO_4 85%, Synth) to form a white-color suspension. At the same time, 3 mmol Iron sulfate ($FeSO_4{\cdot}H_2O$ 99.9%, Xilong chemical Co., Ltd., Shantou, China) was added into beaker B, and then 0.5 mmol of ascorbic acid (99.7%, Xilong chemical Co., Ltd.) was added into beaker B synchronization to protect Fe^{2+} from being oxidized. Next, the mixed solution in beaker B was dropped into beaker A under vigorous magnetic stirring for 30 min, forming an absinthe-green suspension with large amounts of precipitates, and a pH value (approx. 7) for the absinthe-green mixture was controlled by adding hydrazine hydrate solution. Subsequently, the mixture was transferred into a 100 mL Teflon-stainless

autoclave and heated at 180 °C for 18 h. Following, the mixture, after cooling down to room temperature, was centrifuged to obtain the precipitation, and then the precipitation was washed and centrifuged with ethyl alcohol and deionized water for several times to get rid of the remaining ions. The precursors were treated at 700 °C for 6 h in a N_2 atmosphere in a tube furnace with a heating-rate of 3 °C/min to obtain the $LiFePO_4$ electrode materials with OA. To investigate comparatively, the $LiFePO_4$ electrode material was also prepared at the same condition without OA.

2.2. Physiochemical Characterization of $LiFePO_4$

Crystal structures of the micro/nano-structured $LiFePO_4$ electrode materials with grape-like morphology were determined using a Rigaku D/max 2500 pc X-ray diffractometer (XRD), utilizing a Cu Kα radiation source (λ = 0.15406 nm) operated at 40 kV and 30 mA with a step scan of 0.02° (10–80°, 4° min^{-1}). The microstructure and the morphology of the prepared $LiFePO_4$ mounted on a Cu grid were characterized with a JEM-2100 transmission electron microscope (TEM) and S-4800 field-emission scanning electron microscopy (SEM). Raman spectrum was performed on a Renishaw Gloucestershire with a laser wavelength of 514 nm.

2.3. Electrochemical Measurement

The electrochemical performances of the micro/nano-structured $LiFePO_4$ electrode materials with grape-like morphology were measured using two-electrode cells assembled in an Ar-filled glove box. The working electrodes were prepared by mixing the activated material (as-prepared $LiFePO_4$ electrode materials) with acetylene black and polovinylidene fluoride (PVDF) at a mass ratio of 80:15:5 by blending in N-methylpyrrolidone to form a slurry; then, the slurry was spread onto an aluminum foil homogeneously to obtain the working electrode. The as-prepared working electrode was then dried at 120 °C for 12 h in a vacuum drying oven. Lithium foil was used as the anode in a mixture electrolyte solution (1 M $LiPF_6$: ethylene carbonate (EC): diethyl carbonate (DEC) = 1:1:1).

The electrochemical performances of the micro/nano-structured $LiFePO_4$ electrode materials were carried out with a BTS 5 V, 1 A system under different current densities, with voltage ranging from 2.5 to 4.3 V. A cyclic voltammetry (CV) test (scan rate was 0.4 $mV{\cdot}S^{-1}$) was performed. Electrochemical impedance spectroscopy (EIS) was used for measuring the charge transfer resistance (R_{ct}) and investigate the beneficial effect of micro/nano-structured $LiFePO_4$ on battery reaction kinetics. After the test electrodes were completely activated, EIS measurements were conducted on a CHI660E electrochemical workstation with ZPLOT electrochemical impedance software. The EIS spectra of the micro/nano-structured $LiFePO_4$ electrode materials were obtained in a frequency range from 100 kHz to 0.01 Hz with an alternating current amplitude of 5 mV (a sinusoidal excitation voltage of 5 mV). According to the analysis model [22,31], an equivalent circuit for the $LiFePO_4$ electrode materials was used. Using least-square method, the parameters in the equivalent circuit were fitted with ZVIEW electrochemical impedance software. All potentials cited in this paper are referred to Li/Li^+.

3. Results and Discussion

3.1. Characterization of Structure and Morphology

Figure 1 shows the XRD patterns of the as-prepared $LiFePO_4$ cathode materials without and with OA used as the surfactant, respectively. Positions of the Bragg peaks on the XRD pattern of the as-prepared $LiFePO_4$ cathode materials with OA match well with the XRD pattern of the standard diffraction lines of the identified phase, indicating a good phase matching with the $LiFePO_4$ (JCPDS # 40-1499) with an orthorhombic olivine-type structure. In addition, the lattice parameter and cell volume of the $LiFePO_4$ cathode materials are calculated with JADE 5.0 software, respectively, and the results are given in Table 1. We note that those lattice parameters of the $LiFePO_4$ cathode materials prepared with OA are larger than that $LiFePO_4$ cathode materials prepared without OA.

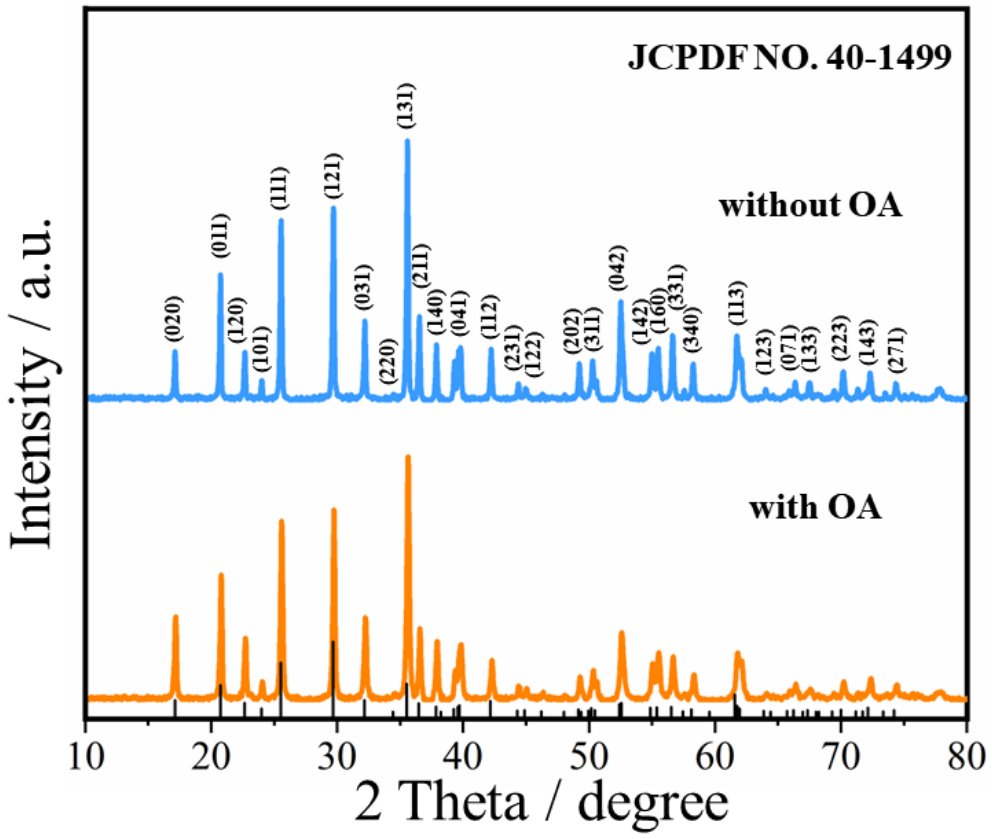


Figure 1. XRD patterns of $LiFePO_4$ prepared without and with OA.

Table 1. Some XRD and electrochemical parameters of the $LiFePO_4$ electrodes prepared without and with OA.

Samples	*a* (nm)	*b* (nm)	*c* (nm)	V (nm^3)	C_{20} ($mAh \cdot g^{-1}$)	C_{-20} ($mAh \cdot g^{-1}$)	R_{ct} (Ω)
without OA	1.0322	0.6002	0.4696	0.2909	133	68	444
with OA	1.0338	0.6007	0.4702	0.2916	161	102	221

C_{20} ($mAh \cdot g^{-1}$): the capacity at 20 °C; C_{-20} ($mAh \cdot g^{-1}$): the capacity at −20 °C; R_{ct} (Ω): the charge–transfer reaction resistance.

Figure 2 is SEM images and TEM images of the $LiFePO_4$ particles prepared. As seen from Figure 2a, the $LiFePO_4$ particles prepared without OA are dispersed with homogeneous single-particles, while the $LiFePO_4$ particles prepared with OA consist of spherical particles with a grape-like morphology (Figure 2b). At higher magnification (see Figure 2c), the grape-like $LiFePO_4$ microspheres are self-assembled by a number of nano particles with an average diameter of about 100 nm. Two peaks were observed on the Raman spectra (inset in Figure 2d). The former is the signal of defective carbon atoms (sp^3-boned, 1340–1350 cm^{-1}) and the latter is the signal of carbon atoms with sp^2-bonded carbon atoms (graphite carbon, 1580–1600 cm^{-1}). It is seen from the inset in Figure 2d that a number of thin film carbon inlaid on the surface of the $LiFePO_4$ particles prepared, which coincides well with Raman's analysis.

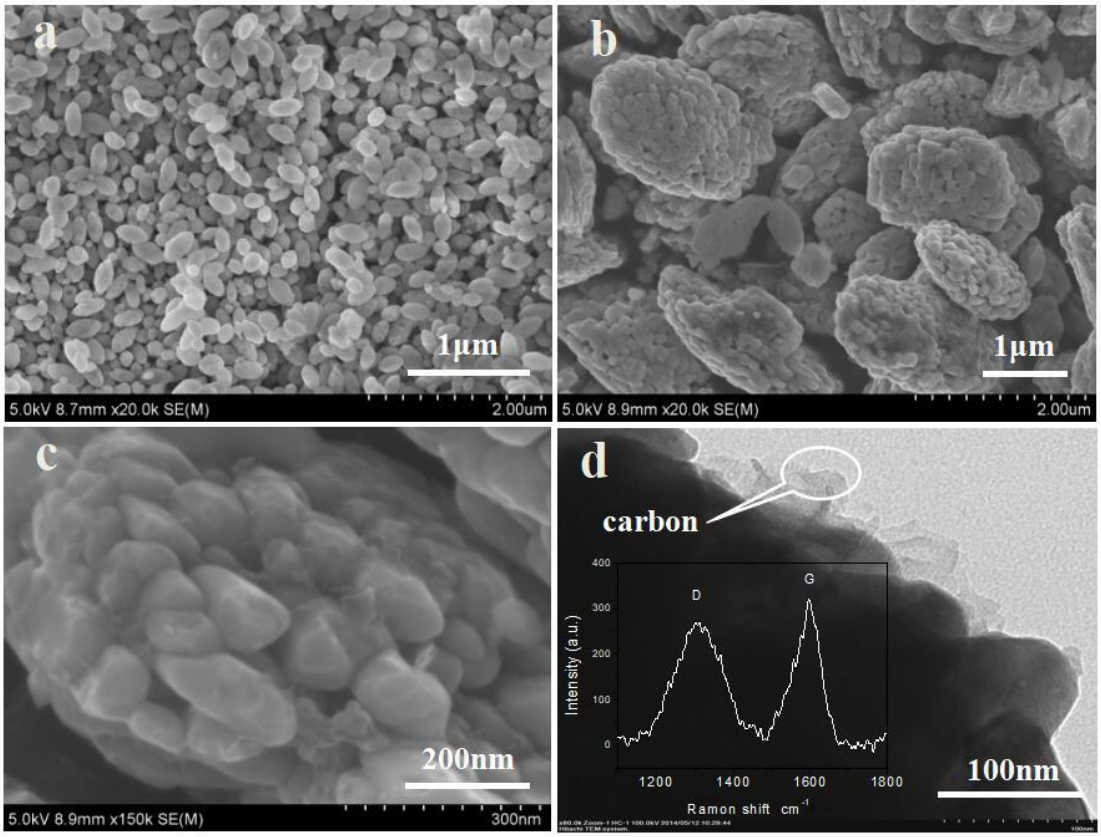


Figure 2. SEM images of $LiFePO_4$ prepared without OA (**a**) and with OA (**b**), high magnification (**c**), TEM with an inset of Raman result $LiFePO_4$ microspheres prepared with OA (**d**).

3.2. Formation Mechanism

To explore the formation mechanism of a grape-like $LiFePO_4$ microsphere, the effect of heating time on the morphology of the micro/nano-structured $LiFePO_4$ electrode material is discussed in more details. Figure 3a–c shows the TEM images of the micro/nano-structured $LiFePO_4$ material synthesized after a certain times. As shown in Figure 3a, the $LiFePO_4$ electrode materials with irregular morphology after 6 h were assembled with a large numbers of $LiFePO_4$ nanocrystals. When the heating time extended to 12 h, the quasi grape-like $LiFePO_4$ microspheres were observed (Figure 3b), and when the heating time extended to 18 h, grape-like $LiFePO_4$ microspheres were observed clearly (Figure 3c).

Xia et al. [22] prepared spindle-like $LiFePO_4$ nanocrystals and investigated the growth mechanism of the $LiFePO_4$, indicating that reaction time and the pH environment played multifold roles in controlling the spindle-like morphology of $LiFePO_4$. In addition, the growth orientation and the grain boundaries were also investigated, indicating that the spindle-like $LiFePO_4$ nanocrystals were assembled with the growth process of $LiFePO_4$ nanocrystals happening simultaneously. Rangappa et al. [30] prepared flower-like $LiFePO_4$ nanocrystals using a solvothermal method with ethylene glycol (EG) and OA as co-solvent and surfactant, where the EG and OA acted as a soft template in directing the growth of $LiFePO_4$ nanocrystals at the early stages and the flower-like structure was self-assembled in the presence of OA. According to the growth mechanism proposed by Rangappa et al., it was the interaction of the adsorbed OA molecules that played an important role in controlling the size and flower-like morphology of $LiFePO_4$ nanocrystals.

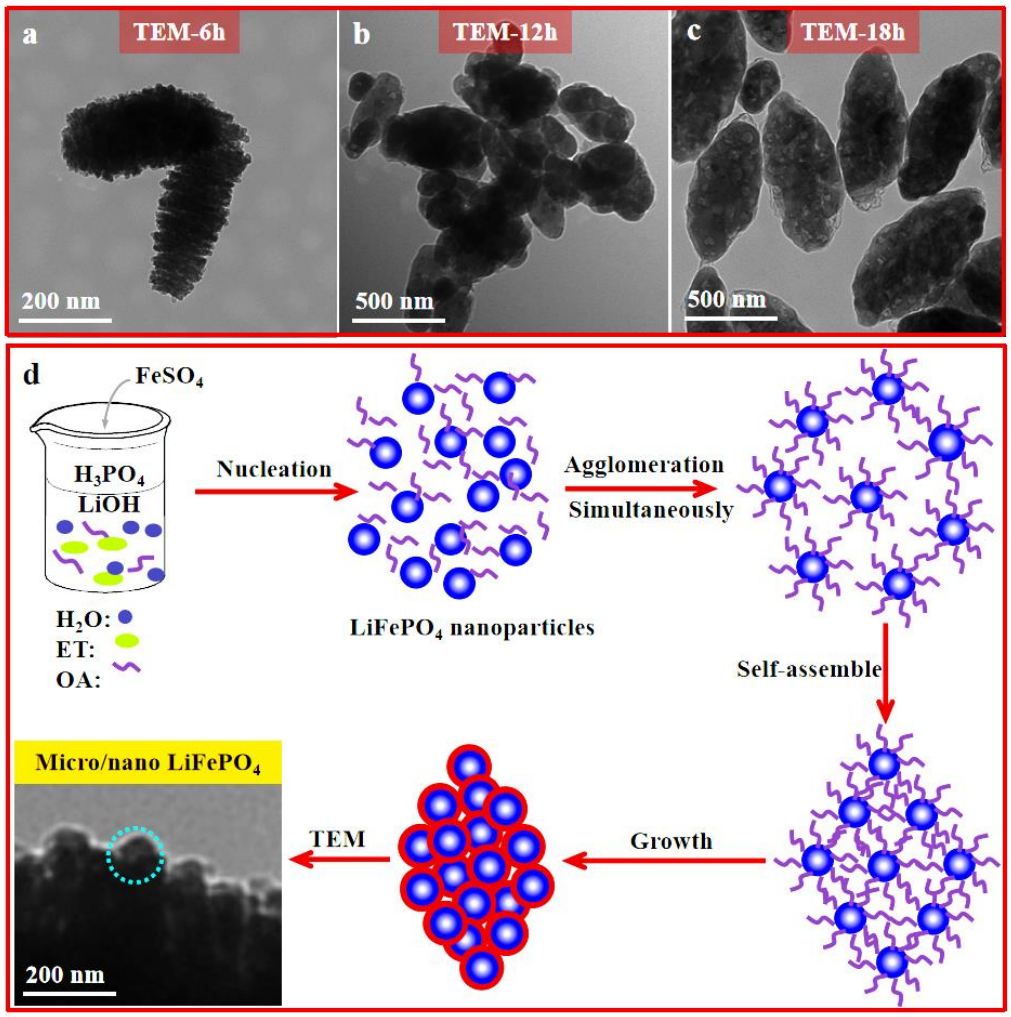


Figure 3. TEM images of $LiFePO_4$ microspheres with OA at 6 h (**a**), 12 h (**b**), 18 h (**c**) and the schematic illustration of formation mechanism of the grape-like $LiFePO_4$ microsphere (**d**).

The formation mechanism of the $LiFePO_4$ microspheres is schematically illustrated in Figure 3d [22,30]. First, $LiFePO_4$ precursor was synthesized with the mixing of the reactants in the co-solvent system; OA, as a typical surfactant, is composed of a hydrophilic head (carbonyl group (C=O)) and a hydrophobic organic tail ($-(CH_2)_7CH{=}CH\ (CH_2)_7CH_3$). Due to the hydrophilic of the $LiFePO_4$ precursor, the hydrophilic head of OA tends to adsorb on the surface of $LiFePO_4$ with the hydrophobic organic tail outward and those hydrophobic organic tails are aggregated after heat treatment. In this work, micro/nano-structured $LiFePO_4$ electrode materials with grape-like morphology were fabricated via a facile solvothermal approach using ethanol and OA as the co-solvent, the surfactant as well as the carbon source, where the OA played a key role in controlling morphology of $LiFePO_4$ nanocrystals.

3.3. Electrochemical Properties

Figure 4a shows the initial charge/discharge profiles for the $LiFePO_4$ electrode prepared without and with OA. As seen from Figure 4a, the $LiFePO_4$ prepared with OA has a specific discharge capacity of 161 $mAh{\cdot}g^{-1}$ at 0.2 C, which is increased by 20.9% in comparison with that of the $LiFePO_4$ synthesized without OA (133 $mAh{\cdot}g^{-1}$).

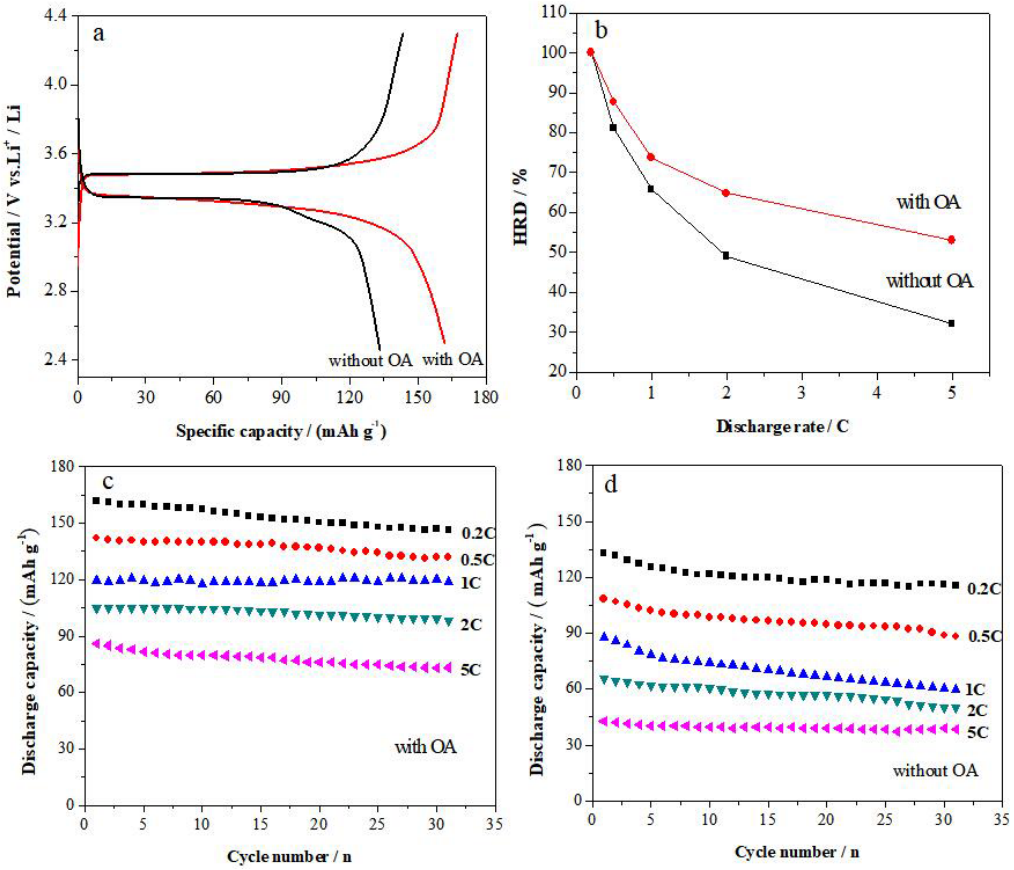


Figure 4. Initial charge/discharge profiles (**a**), the HRD (**b**), cycle performance of $LiFePO_4$ electrodes prepared with OA (**c**) and without OA (**d**).

The relationship between the discharge capacity and the discharge current density of the $LiFePO_4$ cathode materials at 0.2 C, 0.5 C, 1 C, 2 C and 5 C is shown in Figure 4b. It is learnt from Figure 4b that the high-rate discharge capacity (HRD) of the $LiFePO_4$ cathode materials prepared with OA is 142, 119, 105 and 86 at 0.5 C, 1 C, 2 C and 5 C, which is about 31%, 36%, 61% and 101% higher than that of $LiFePO_4$ materials prepared without OA, respectively. Figure 4c,d depicts the cycling stability at 0.2 C, 0.5 C, 1 C, 2 C and 5 C of the $LiFePO_4$ cathode materials. It is obvious that all the capacity retention at 30 times charge/discharge cycles exceeds 90%.

Figure 5 shows the specific discharge capacity of the $LiFePO_4$ electrode prepared at the temperatures ranging from −40 °C to 50 °C. Evidently, the $LiFePO_4$ cathode materials prepared with OA has higher discharge capacity than that without OA at all the temperatures. At 0 °C, −10 °C, −20 °C and −40 °C, the specific discharge capacity is 142 $mAh{\cdot}g^{-1}$, 125 $mAh{\cdot}g^{-1}$, 102 $mAh{\cdot}g^{-1}$ and 87 $mAh{\cdot}g^{-1}$, which is respectively 88%, 78%, 63% and 54% when compared with the specific discharge capacity of 161 $mAh{\cdot}g^{-1}$ at the ambient temperature (20 °C).

Figure 6 shows the cyclic voltammetry (CV) curves of the samples at the scan rate of 0.4 $mV{\cdot}S^{-1}$ after activation for 2 cycles. It can be seen from Figure 6 that the oxidation peaks and reduction peaks of the sample prepared with OA appear at 3.27 V and 3.61 V with a gap of 0.34 V, which is less than that of the sample prepared without OA (0.57 V).

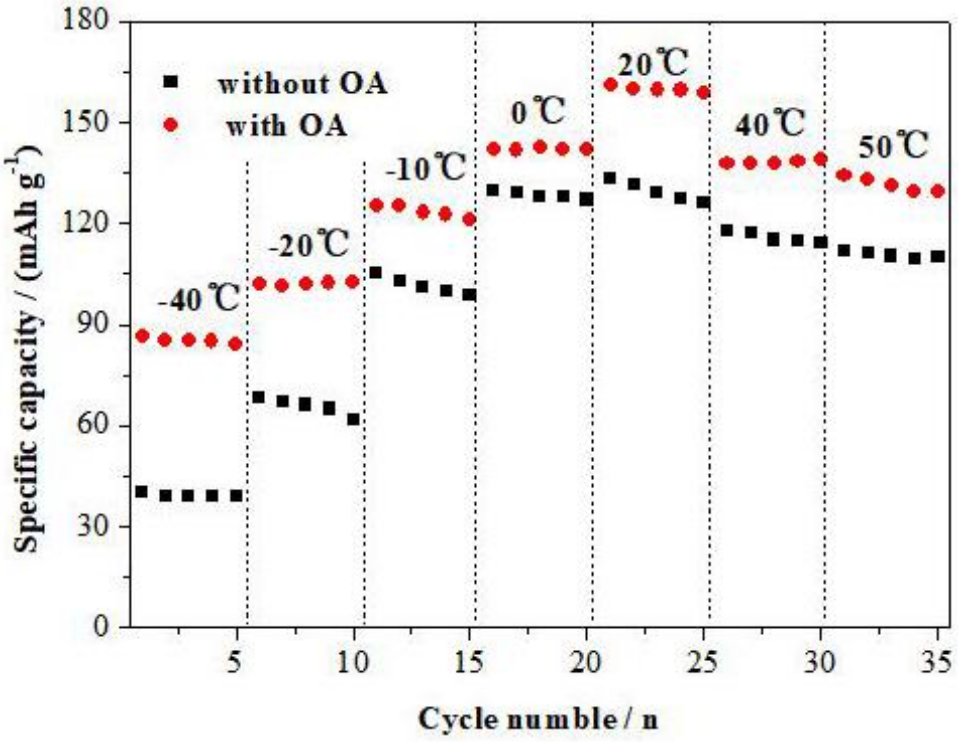


Figure 5. Effect of temperature on the specific capacity of $LiFePO_4$ electrodes prepared.

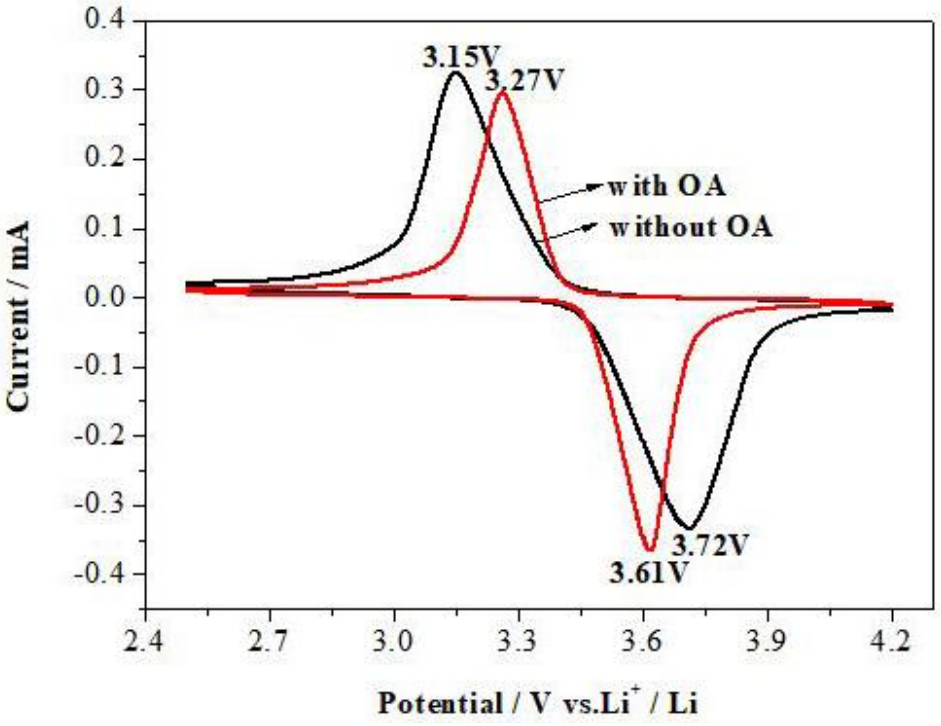


Figure 6. Cyclic voltametric profiles of $LiFePO_4$ electrodes prepared.

To further examine the electrode's behavior of the micro/nano-structured $LiFePO_4$, EIS measurements were performed and the EIS spectra of the micro/nano-structured $LiFePO_4$ electrode materials were obtained in a frequency range from 100 kHz to 0.01 Hz (Figure 7). An equivalent circuit for the micro/nano-structured $LiFePO_4$ electrode materials was used to analyze the impedance spectra (inset in Figure 7a), where the R_s, R_{ct}, CPE and W_o represent the resistance of the electrolyte (R_s), the charge–transfer resistance (R_{ct}),

the double-layer capacitance and the Warburg impedance, respectively. In high frequency, an intercept at the Z′ axis was used to evaluate the R_s. In the high-middle frequency, the semicircle was used to evaluate the R_{ct}. In the low frequency, the inclined line was used to evaluate the W_o, which was attributed to the diffusion of Li ion into the micro/nano-structured $LiFePO_4$ electrode materials. The equivalent capacitance is used to describe the electric double layer between the electrode and the solution. However, the impedance behavior of the solid electrode's electric double layer deviates somewhat from that of the equivalent capacitance. This phenomenon is generally called "dispersion effect". The dispersion effect caused by the material surface inhomogeneity of micro/nano structures is called constant phase angle element (CPE). The CPE is related to changes in the thickness, roughness and porosity of the electrode material. The fitting result indicates that the value of R_s is 5.3 Ω for the micro/nano-structured $LiFePO_4$ electrode, which is about 43% lower than that of $LiFePO_4$ electrode prepared without OA, indicating a smaller resistance of the electrolyte. The fitting result indicates that the value of R_{ct} is 221 Ω for the micro/nano-structured $LiFePO_4$ electrode, which is about 50% lower in comparison with that of the $LiFePO_4$ electrode materials prepared without OA (444 Ω) (Figure 7a, Table 2). Meanwhile, we add bode plots to support the discussion on Nyquist diagrams (Figure 7b,c). In addition, the straight line in low frequency was attributed to the diffusion of li ion into the bulk of the $LiFePO_4$ electrode materials, where the slope of the straight line represented the Warburg impedance. It is observed that the Warburg impedance of the micro/nano-structured $LiFePO_4$ electrode materials is higher in comparison with the other $LiFePO_4$ electrode materials. The parameters of the equivalent circuit for the micro/nano-structured $LiFePO_4$ electrode materials and the $LiFePO_4$ electrode materials prepared without OA were recorded in Table 1.

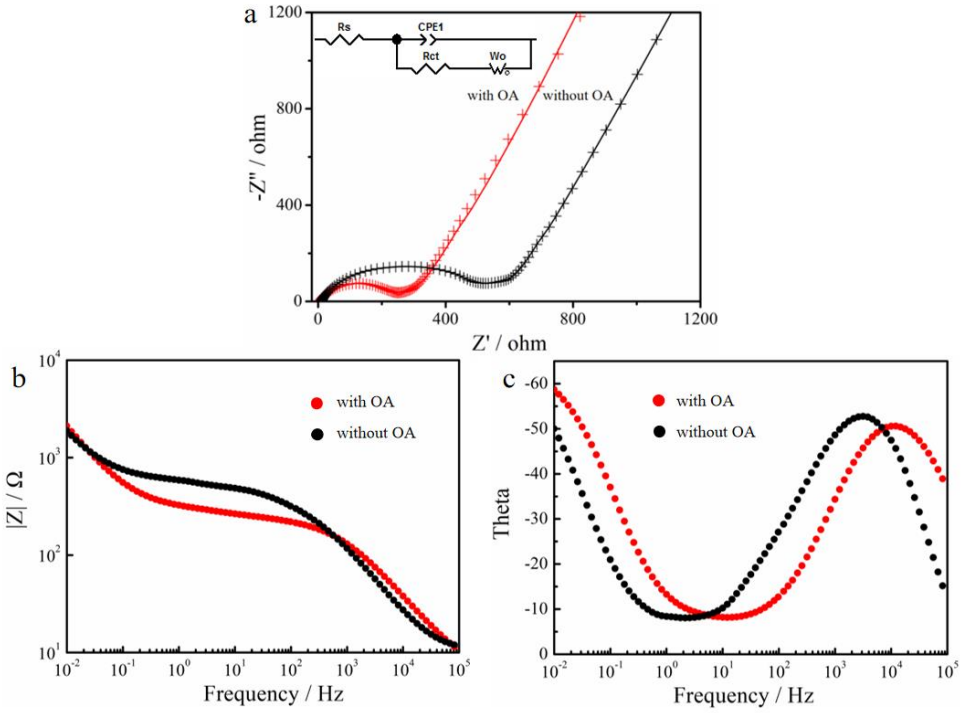


Figure 7. Impedance spectra profiles of $LiFePO_4$/C electrodes prepared. (**a**) Nyquist diagrams (The inset is an equivalent circuit diagram). (**b**,**c**) Bode plots.

Table 2. The specific values of each parameter in the equivalent circuit.

	R_s	CPE	R_{ct}	Chi-Squared
with OA	5.3	8.7×10^6	221	9.7×10^4
without OA	9.3	1.3×10^5	444	1.7×10^3

4. Conclusions

In this investigation, micro/nano-structured $LiFePO_4$ electrode materials with grape-like morphology were fabricated via a facile solvothermal approach using mixture of ethanol/water/oleic acid as a co-solvent and oleic acid (OA) as a surfactant. We note that those lattice parameters of the $LiFePO_4$ cathode materials prepared with OA are larger than that $LiFePO_4$ cathode materials prepared without OA. The micro/nano-structured $LiFePO_4$ electrode materials exhibited a high discharge capacity of 142 $mAh{\cdot}g^{-1}$ at 0 °C, and retained 102 $mAh{\cdot}g^{-1}$ when the temperature was decreased to −20 °C. The micro/nano-structured $LiFePO_4$ electrode materials revealed a lower charge–transfer resistance, indicating an improved dynamic performance of li-ion diffusion.

Author Contributions: Conceptualization, P.J. and T.J.; data curation, Y.Q., Y.L., J.Z., L.Z. and W.Z.; writing—original draft preparation, Y.Q.; writing—review and editing, T.J. All authors have read and agreed to the published version of the manuscript.

Funding: This work was supported by the National Natural Science Foundation of China (grants 2227911 and 11935004), the Natural Science Foundation of Hebei Province (B2020203037 and B2021203016), the China Postdoctoral Science Foundation (2021M702756), and the Special Project for Local Science and Technology Development, guided by the central government of China (216Z1301G and 226Z1401G).

Institutional Review Board Statement: Not applicable.

Informed Consent Statement: Not applicable.

Data Availability Statement: Data presented in this article are available on request from the corresponding author.

Conflicts of Interest: The authors declare that they have no conflict of interest.

References

1. Chen, S.P.; Lv, D.; Chen, J.; Zhang, Y.H.; Shi, F.N. Review on defects and modification methods of $LiFePO_4$ cathode material for lithium-ion batteries. *Energ. Fuel.* **2022**, *36*, 1232–1251. [CrossRef]
2. Huang, C.Y.; Kuo, T.R.; Yougbaré, S.; Lin, L.Y. Design of $LiFePO_4$ and porous carbon composites with excellent High-Rate charging performance for Lithium-ion secondary battery. *J. Colloid Interf. Sci.* **2022**, *607*, 1457–1465. [CrossRef] [PubMed]
3. Kumar, J.; Neiber, R.R.; Park, J.; Soomro, R.A.; Greene, G.W.; Mazari, S.A.; Seo, H.Y.; Lee, J.H.; Shon, M.; Chang, D.W.; et al. Recent progress in sustainable recycling of $LiFePO_4$-type lithium-ion batteries: Strategies for highly selective lithium recovery. *Chem. Eng. J.* **2022**, *43*, 133993. [CrossRef]
4. Liang, J.L.; Gan, Y.H.; Yao, M.L.; Li, Y. Numerical analysis of capacity fading for a $LiFePO_4$ battery under different current rates and ambient temperatures. *Int. J. Heat Mass Tran.* **2021**, *165*, 120615. [CrossRef]
5. Lin, J.; Sun, Y.H.; Lin, X.M. Metal-organic framework-derived $LiFePO_4$ cathode encapsulated in O, F-codoped carbon matrix towards superior lithium storage. *Nano Energy* **2022**, *91*, 106655. [CrossRef]
6. Sanchez, J.S.; Xu, J.; Xia, Z.Y.; Sun, J.H.; Asp, L.E.; Palermo, V. Electrophoretic coating of $LiFePO_4$/graphene oxide on carbon fibers as cathode electrodes for structural lithium ion batteries. *Compos. Sci. Technol.* **2021**, *208*, 108768. [CrossRef]
7. Zhang, H.W.; Li, J.Y.; Luo, L.Q.; Zhao, J.; He, J.Y.; Zhao, X.X.; Liu, H.; Qin, Y.B.; Wang, F.Y.; Song, J.J. Hierarchically porous MXene decorated carbon coated $LiFePO_4$ as cathode material for high-performance lithium-ion batteries. *J. Alloys Compd.* **2021**, *876*, 160210. [CrossRef]
8. Scrosati, B. Recent advances in lithium ion battery materials. *Electrochim. Acta* **2000**, *45*, 2461–2466. [CrossRef]
9. Wang, J.W.; Liu, J.; Yang, G.L.; Zhang, X.F.; Yan, X.D.; Pan, X.M.; Wang, R.S. Electrochemical performance of $Li_3V_2(PO_4)_3$/C cathode material using a novel carbon source. *Electrochim. Acta* **2009**, *54*, 6451–6454. [CrossRef]
10. Hu, W.; Zhang, X.B.; Cheng, Y.L.; Wu, Y.M.; Wang, L.M. Low-cost and facile one-pot synthesis of pure single-crystalline ε-$Cu_{0.95}V_2O_5$ nanoribbons: High capacity cathode material for rechargeable Li-ion batteries. *Chem. Commun.* **2011**, *47*, 5250–5252. [CrossRef]
11. Ma, D.L.; Cao, Z.Y.; Wang, H.G.; Huang, X.L.; Wang, L.M.; Zhang, X.B. Three-dimensionally ordered macroporous FeF_3 and its in situ homogenous polymerization coating for high energy and power density lithium ion batteries. *Energy Environ. Sci.* **2012**, *5*, 8538. [CrossRef]
12. Wang, H.G.; Ma, D.L.; Huang, Y.; Zhang, X.B. Electrospun V_2O_5 nanostructures with controllable morphology as high-performance cathode materials for Lithium-ion batteries. *Chem. Eur. J.* **2012**, *18*, 8987–8993. [CrossRef] [PubMed]
13. Li, Y.; Wang, L.; Zhang, K.Y.; Liang, F.; Yao, Y.C.; Kong, L.X. High performance of $LiFePO_4$ with nitrogen and phosphorus dual-doped carbon layer for lithium-ion batteries. *J. Alloys Compd.* **2021**, *890*, 161617. [CrossRef]

14. Luo, Z.H.; Zhang, R.L.; Xu, F.F.; Gao, Y.; Zhao, J.S. Structure and electrochemical performance of $LiFePO_4$ cathode materials modified with carbon coating and metal doping. *J. Solid State Electrochem.* **2022**, *26*, 1655–1665.
15. Somo, T.R.; Mabokela, T.E.; Teffu, D.M.; Sekgobela, T.K.; Ramogayana, B.; Hato, M.J.; Modibane, K.D. A comparative review of metal oxide surface coatings on three families of cathode materials for lithium ion batteries. *Coatings* **2021**, *11*, 744. [CrossRef]
16. Zhuang, Y.; Zhang, W.; Bao, Y.Q.; Guan, M.Y. Influence of the $LiFePO_4$/C coating on the electrochemical performance of Nickel-rich cathode for lithium-ion batteries. *J. Alloys Compd.* **2022**, *898*, 162848. [CrossRef]
17. Gao, Y.; Xiong, K.; Zhang, H.D.; Zhu, B.F. Effect of Ru doping on the properties of $LiFePO_4$/C cathode materials for lithium-ion batteries. *ACS Omega* **2021**, *6*, 14122–14129. [CrossRef]
18. Xin, Y.M.; Xu, H.Y.; Ruan, J.H.; Li, D.C.; Wang, A.G.; Sun, D.S. A Review on application of $LiFePO_4$ based composites as electrode materials for Lithium ion batteries. *Int. J. Electrochem. Sci.* **2021**, *16*, 210655. [CrossRef]
19. Zhang, B.F.; Xu, Y.L.; Wang, J.; Ma, X.N.; Hou, W.Q.; Xue, X. Electrochemical performance of $LiFePO_4$/graphene composites at low temperature affected by preparation technology. *Electrochim. Acta* **2021**, *368*, 137575. [CrossRef]
20. Peng, L.L.; Zhao, Y.; Ding, Y.; Yu, G.H. Self-assembled $LiFePO_4$ nanowires with high rate capability for Li-ion batteries. *Chem. Commun.* **2014**, *50*, 9569. [CrossRef]
21. Zhao, Y.; Peng, L.L.; Liu, B.R.; Yu, G.H. Single-crystalline $LiFePO_4$ nanosheets for high-rate Li-ion batteries. *Nano Lett.* **2014**, *14*, 2849–2853. [CrossRef] [PubMed]
22. Xia, Y.; Zhang, W.K.; Huang, H.; Gan, Y.P.; Tian, J.; Tao, X.Y. Self-assembled mesoporous $LiFePO_4$ with hierarchical spindle-like architectures for high-performance lithium-ion batteries. *J. Power Sources* **2011**, *196*, 5651–5658. [CrossRef]
23. Li, Y.C.; Xing, B.Y.; Liang, P.C.; Zhang, H.S.; Zhou, K.Y.; Ma, J.J.; Fan, S.M.; Yang, S.T. Synthesis of graphene-supported $LiFePO_4$/C materials via solid-state method using $LiFePO_4$ (OH) as precursors. *J. Solid State Electrochem.* **2022**, *26*, 2595–2600. [CrossRef]
24. Bezerra, C.A.G.; Davoglio, R.A.; Biaggio, S.R.; Bocchi, N.; Rocha-Filho, R.C. High-purity $LiFePO_4$ prepared by a rapid one-step microwave-assisted hydrothermal synthesis. *J. Mater. Sci.* **2021**, *56*, 10018–10029. [CrossRef]
25. Sellami, M.; Barre, M.; Dammak, M.; Toumi, M. Local structure, thermal, optical and electrical properties of $LiFePO_4$ polycrystalline synthesized by Co-precipitation method. *Braz. J. Phys.* **2021**, *51*, 1521–1528. [CrossRef]
26. Alsamet, M.A.M.M.; Burgaz, E. Synthesis and characterization of nano-sized $LiFePO_4$ by using consecutive combination of sol-gel and hydrothermal methods. *Electrochim. Acta* **2021**, *367*, 137530. [CrossRef]
27. Cao, H.; Wen, L.; Guo, Z.Q.; Piao, N.; Hu, G.J.; Wu, M.J.; Li, F. Application and prospects for using carbon materials to modify lithium iron phosphate materials used at low temperatures. *New Carbon Mater.* **2022**, *37*, 46–58. [CrossRef]
28. Ren, X.; Li, Z.F.; Cao, J.R.; Tian, S.Y.; Zhang, K.C.; Guo, J.L.; Wen, L.Z.; Liang, G.C. Enhanced rate performance of the mortar-like $LiFePO_4$/C composites combined with the evenly coated of carbon aerogel. *J. Alloys Compd.* **2021**, *867*, 158776. [CrossRef]
29. Yang, Z.; Cao, G.S.; Xie, J.; Zhao, X.B. Oleic acid-assisted preparation of LiMnPO4 and its improved electrochemical performance by Co doping. *J. Solid State Electrochem.* **2012**, *16*, 1271–1277. [CrossRef]
30. Rangappa, D.; Sone, K.; Kudo, T.; Honma, I. Directed growth of nanoarchitectured $LiFePO_4$ electrode by solvothermal synthesis and their cathode properties. *J. Power Sources* **2010**, *195*, 6167–6171. [CrossRef]
31. Yi, D.W.; Cui, X.M.; Li, N.L.; Zhang, L.; Yang, D.Y. Enhancement of electrochemical performance of $LiFePO_4$/C by Ga coating. *ACS Omega* **2020**, *5*, 9752–9758. [CrossRef] [PubMed]